IOP Conf. Series: Materials Science and Engineering **779** (2020) 012032 doi:10.1088/1757-899X/779/1/012032

Electro-hydromechanical processes in mineral oil flow

V Pilgunov[1] and K Efremova[1,2]

[1]Bauman Moscow State Technical University

[2]E-mail: efremova.k.d@gmail.com

Abstract: The results of experimental studies of electrical processes occurring in the mineral oils in narrow channels and slots of hydraulic devices are considered. The theoretical substantiation of the detected phenomena is given.

Introduction

In hydraulic devices of automatic type various types of throttles are widely used as shut-off and control elements [1]. In diaphragm throttles the flow of the pressure fluid has a pronounced turbulent character and high speed causes cavitation and the associated release of bubbles of undissolved air and steam in narrow section. Linear and angular deformations of a liquid particle can lead to its polarization. In the flow of a moving at high speed fluid can occur the concentration of energy at which there are local flows with kinetic energy significantly exceeding the average flow energy values [2–4]. When studying the flow of mineral oil in transparent models of a diaphragm throttle at its inlet edge, localized stable light emission was detected in the blue part of the color spectrum which was called hydrodynamic luminescence [5–8]. The brightness of light emission increased during the speed increasing and stopped to change achieving of certain value of the Reynolds number. As there is a limited amount of information about light emission in the cavitation zone at low pressure on the sharp part of the sharp inlet edge of hole in scientific and technical literature [9–15], the additional studies in order to clarify the physical and physic-chemical effects and nature of light emission in a flow of dielectric liquid in narrow slots were conducted.

An experimental study of electro-hydromechanical processes in a flow of mineral oil

Photos of the studied transparent models of throttles are presented in Fig. 1. Models were manufactured of polished organic glass with pronounced dielectric properties. The diameter and width of the diaphragm control throttle hole were 1 mm and 0,5 mm. The pressure fluid was mineral oil brand "SHELL - 20".

The parameters characterizing the fluid motion in the flow cross sections in the diaphragm and capillary throttles are presented in Fig. 2.

For quantitative estimation of the electrical processes in the throttle sections a string manufactured of nickel-chromium wire with diameter of 0,05 mm in three-layer enamel insulation was stretched along its axis (Fig. 1a).

A local stripping of enamel insulation was performed on the string as a result of which a mark with width of 0,1 mm was obtained which provided detection of the electric potential in the selected flow section. A string with mark was extended along the axis of the channel by tension device (Fig. 3) and detected electrical signals in the flow cross sections.

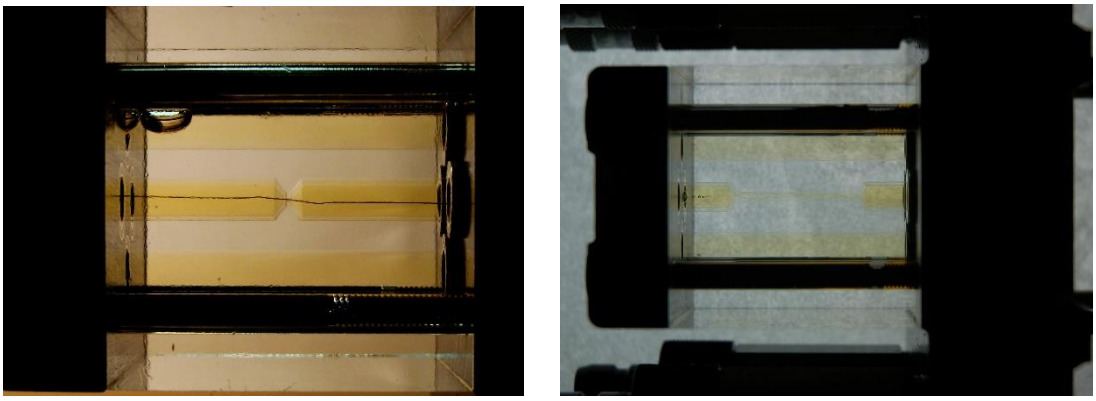

Figure 1. The tested models of throttles
a) Diaphragm throttle b)Capillary throttle

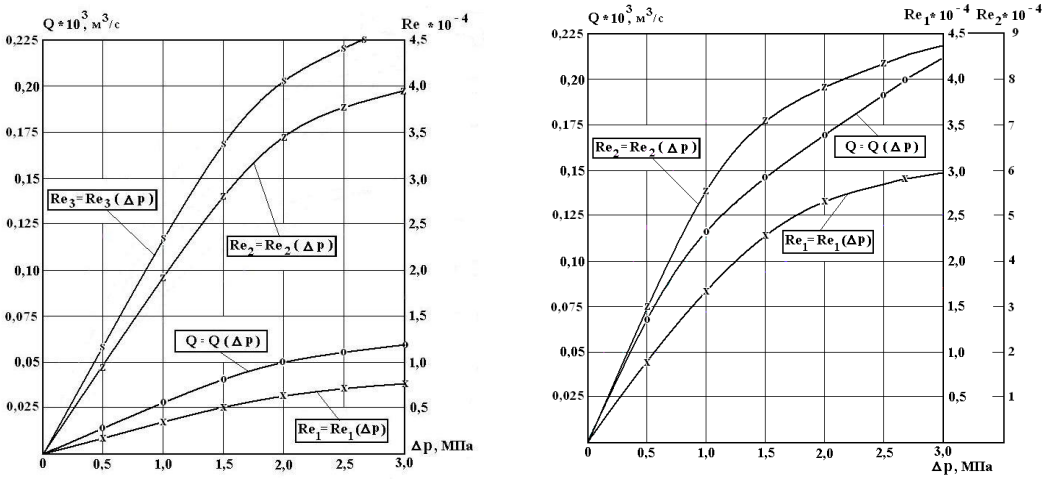

a) Diaphragm throttle b) Capillary throttle

Figure 2. Flow parameters in throttle modules

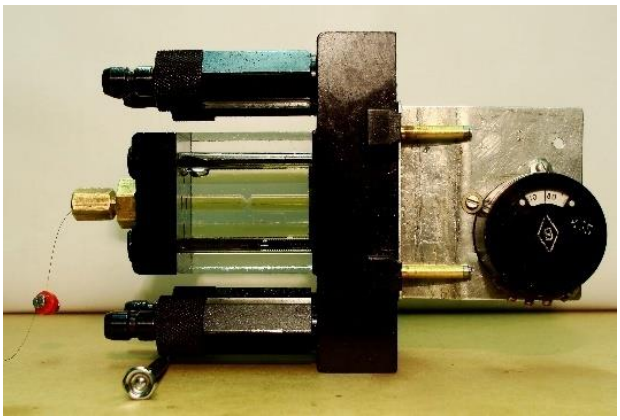

Figure 3. String tension device and mark position recorder

High-frequency electrical signals of complex shape in the flow cross sections were detected (Fig. 4).

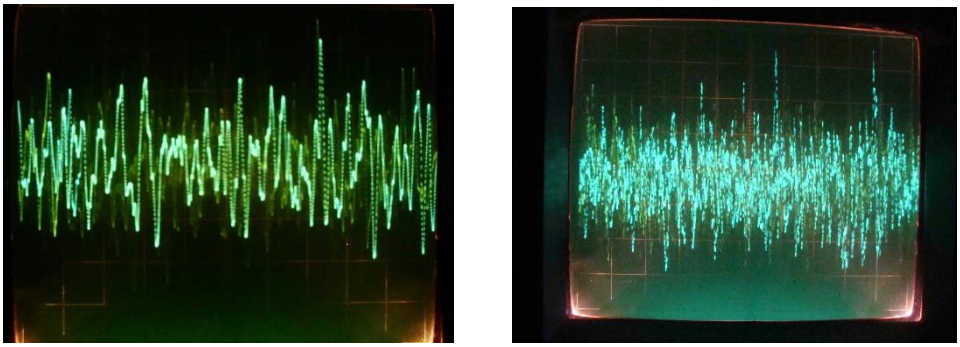

a) Strong string tension b) Released string tension

Figure 4. The shape of the electrical signal at the input edge of the diaphragm control throttle

The numerical results of electrical signals in the flow cross sections are presented in the summary diagram on Fig. 5. Positions of marks 1, 2, 3, 4 and 5 correspond to sections of the throttle module “inlet”, “light emission”, “cavitation core”, “cavitation flare” and “outlet”.

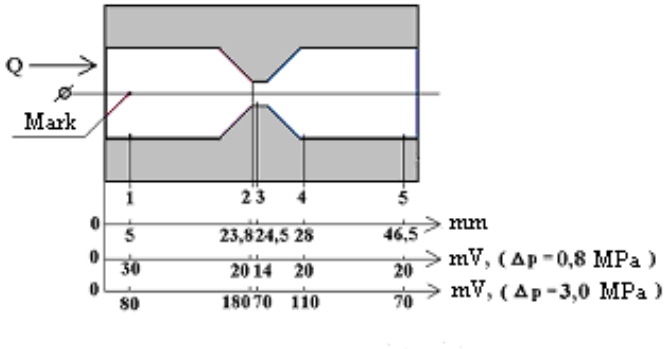

Figure 5. The span of the electrical signals in the flow cross sections

The integrated spectral characteristic of electrical signals was studied using a spectrum analyzer (Fig. 6).

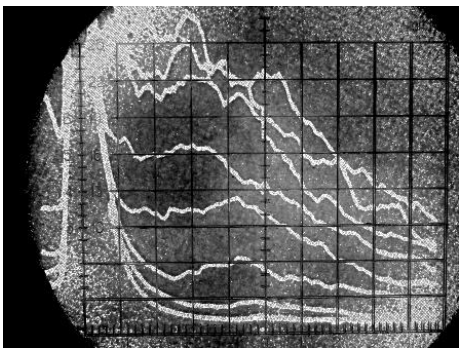

Figure 6. The spectrograms of electrical signal on the inlet edge of the throttle

Spectrograms were recorded at various inlet pressure valuesp_1 = 1.0; 1.5; 2.0; 2.5; 3.0; 4.0 MPa: the lower lines in the spectrograms correspond to the minimum pressure values, the upper lines – to the maximum. The frequency spectrum of the signals is in the range D_f = 2 ... 10 kHz. In cold mineral oil in the cross section along the input edge of the throttle the integrated voltage value at a frequency of

2 kHz reached a maximum value of U_{2kHz} = 200 mV. Heating the oil to t^0C = + 50^0C caused a decrease of the voltage integrated value at this frequency on the average in 1.5 times.

Significant span of electrical signals detected in the inlet and outlet of the diaphragm throttle necessitated the study of a cavitation-free flow of mineral oil in the capillary throttle (inlet diameter d_p = 6 mm, diameter of the capillary d_c = 2 mm (Fig. 1b). The velocity of the fluid in the capillary wasV_2 = 70 m / s. The shape of the electric signal in the middle of the length of the capillary is shown in Fig. 7.

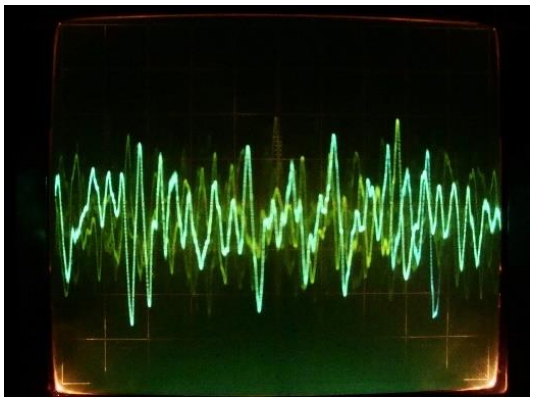

Figure 7. The shape of the electric signal in the middle of the length of the capillary throttle

Corrected span values of electrical signal are shown on summary diagram in Fig.8.

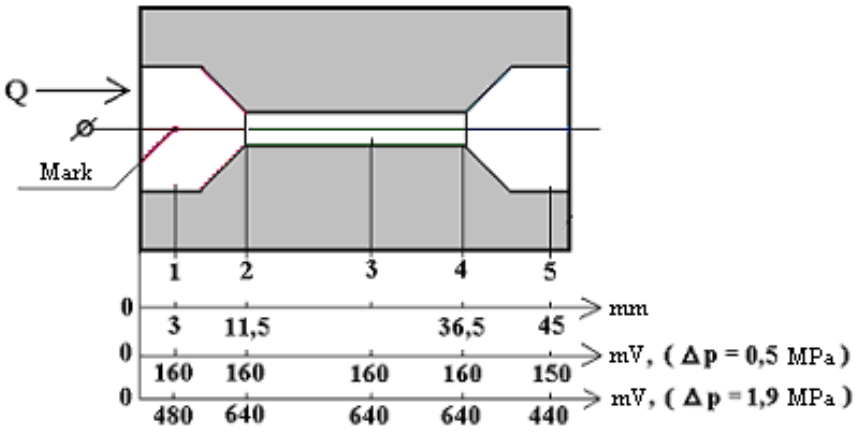

Figure 8. Span values of electrical signal of capillary throttle cross sections

The frequency spectrum of the signals is in the range D_f = 2 ... 10 kHz. In the inlet, the value of the integral voltage is slightly higher than in the outlet which caused by the loss of voltage along the length of the channel. In order to find out the reasons for the presence of electrical processes in the mineral oil flow and the influence of the material of the channel walls on them a model of a combined throttle was manufactured (Fig. 9) in which the inlet and diaphragm throttle were manufactured of brass (CuZn) and grounded.

The corrected signal spans presented in the summary diagram (Fig. 10). From the diagram it follows that the electrical signal reaches its maximum value of 270 mV at the entrance to the capillary (section 3).

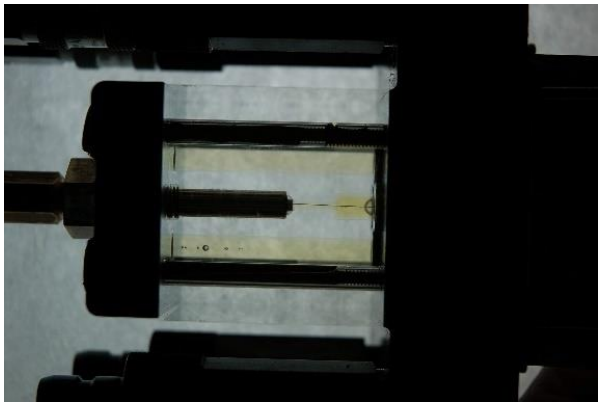

Figure 9. Combined throttle

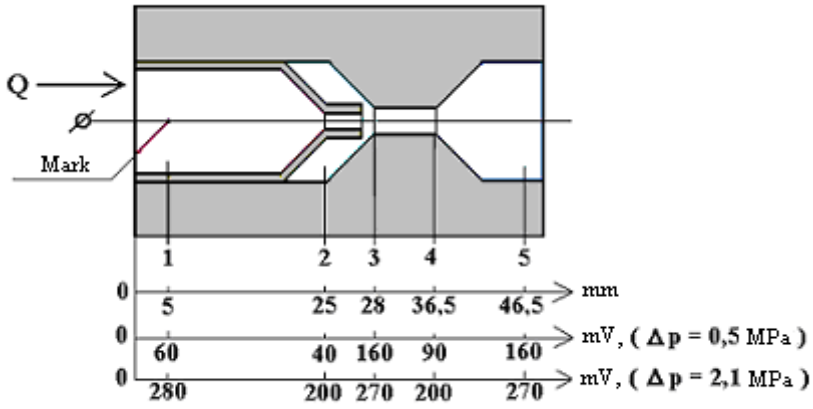

Figure 10. Signal span in the combined throttle cross sections

The occurrence of significant charges in the inlet channel indicates that the detected electrical processes are not associated with friction during the relative movement of two dielectrics.

For a more detailed study of electro-hydromechanical processes in the flow of a dielectric fluid a module was studied in which a metal plain washer was installed with a round hole with diameter of 0.9 mm with sharp inlet edge (Fig. 11).

Figure 11. Module with a metal plain washer

The researches were carried out at the experimental test bench (Fig. 12).

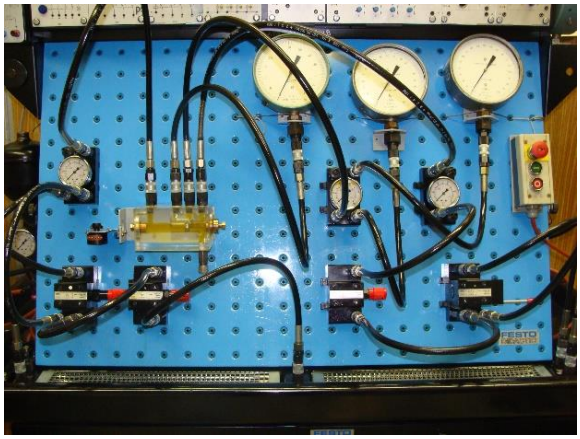

Figure 12. The experimental test bench for the study of a module with a metal plain washer

The electro-hydromechanical processes in the module were quite intense (Fig. 13).

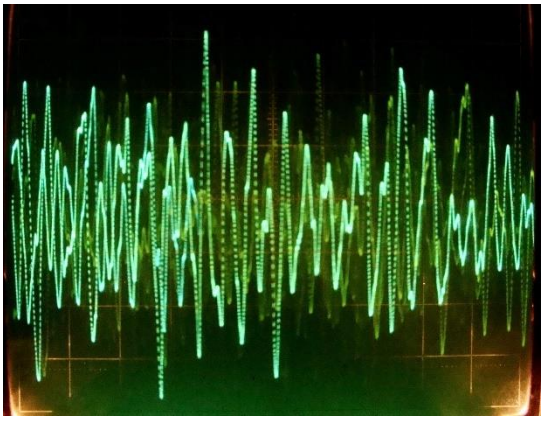

Figure 13. Oscillogram of electrical signals in a module with a metal plain washer

The corrected span values of electrical signal are presented in the summary diagram (Fig. 14).

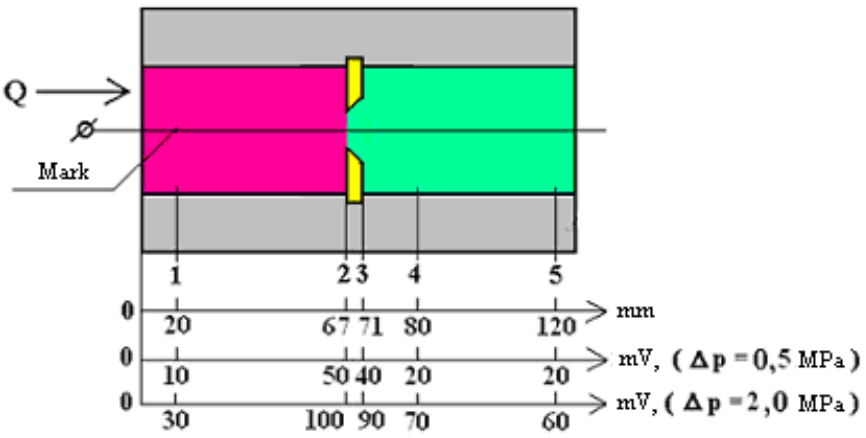

Figure 14. Span values of electrical signals in module with a metal plain washer

Discussion of the experimental results

An analysis of oscillograms and spectrograms allows us to establish the occurrence of electrical processes in the flow of mineral oil which are observed both in the inlet channels and in local compressions of the flow (diaphragm and capillary throttles) while their occurrence does not depend on the material of the walls restricting the flow. The frequency range of electrical signals is in the range D_f = 2 ... 10 kHz while low frequencies are more intense (Fig. 6). It can be assumed that in a metallized inlet channel a thin laminar sub layer of a dielectric fluid plays the role of insulation. The spectral characteristics (Fig. 7) indicate that the Reynolds number has a significant effect on the intensity of electrical processes. In accordance with the data given in [16–21], a double electric layer forms at the interface between two media ("solid wall - flow of dielectric fluid")which is a common property of dielectric fluids [22–24]. The fluid motion in a narrow channel can be considered in the OXYZ 3-coordinate system in which the origin of coordinates is associated with an arbitrary point on a solid interface between two media, the X axis is directed normal to the interface towards the flow, the Y axis is parallel to the tangent to the interface and the "Z" axis is parallel to the main flow vector (Fig. 15). The solid wall has an electric potential equal to the thermodynamic potential φ_T. The dense part of the double electric layer with thickness of Xc equal to 5 ... 10 molecular diameters ("sliding boundary") borders the interface between the two media.

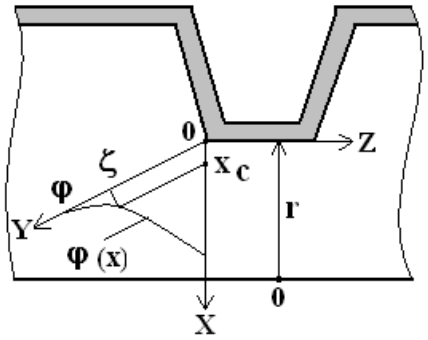

Figure 15. Binding OXYZ 3-coordinate system

In the remote from the interface surface of the diffuse part of the double electric layer ions can freely move and be carried away by the fluid flow. At values of $X < X_c$ single electric charges can only move together with the surface layer. After flushing the diffuse layer by the liquid flow these charges form an uncompensated electric charge on the interface between the two media.

According to the Poisson equation the distribution of the density of the electric charge in a dielectric fluid is determined by the following expression:

$$\rho(x) = -\varepsilon_a \cdot \varepsilon_o \left(\frac{\partial^2 \varphi}{\partial x^2} \right) = -\varepsilon \cdot \varepsilon_o^2 \left(\partial^2 \varphi / \partial x^2 \right), \quad (1)$$

where ε_a — absolute dielectric constant, $\varepsilon = \varepsilon_a / \varepsilon_o$ — relative dielectric constant, $\varepsilon_0 = 8.85 \times 10^{-12}$ $F \cdot m^{-1}$ (Farads per meter)–vacuum permittivity(epsilon zero).

In accordance with Newton's law of viscous friction the velocity distribution of elementary streams over the flow cross section is determined by the equality:

$$V(X) = F(X - X_c) / 2\pi\mu r L, \quad (2)$$

where F — Newton's force of friction, μ — dynamic fluid viscosity, r — inner radius of the channel, L — channel length. In the laminar sub layer at the interface between two media the transverse velocity gradient dV /dX and the force F are almost constant. From equality (2) follows the expression for the force F:

$$F = 2\pi\mu r\, LV(X)/(X - X_c). \quad (3)$$

The amount of electricity carried by the diffuse layer per unit time is determined by the double integral over the surface:

$$I = \iint_{(S)} V(X)\rho(x)dX\, dY, \quad (4)$$

where (S) — is the area of the "real" section of the stream. Taking into account equalities (1) and (2) equation (4) is equated to following expression:

$$I = \left(\varepsilon \cdot \varepsilon_0^2 F / 2\pi\mu rL\right) \int_{0\ldots 2\pi r} dY \int_{Xc}^{X} X\left(\frac{d^2\varphi}{dX^2}\right)dX. \quad (5)$$

If we take into account that the first integral within the integration limit 0 ... 2πr takes the value equal to 2πr and the second integral within the integration limit from X = Xc to X = r is equal to the "zeta potential" ς, then equality (5) is significantly simplified and takes the form

$$I = \varepsilon \cdot \varepsilon_o^2\ F\zeta / \mu L. \quad (6)$$

The equation of the dynamics of the flow flushing the diffuse part of the double electric layer, taking into account equality (3) and the smallness of the slip boundary $X_c << r$ is determined by the expression:

$$F = 2\pi\mu r\, LV(X/(X\ Xc) = \pi r^2 \Delta p, \quad (7)$$

where Δp — is the pressure drop across the areas of the "real" cross sections of the flow flushing the diffuse layer.

After substitution the value of Newton's force in equality (6) get the following equation:

$$I = \pi\varepsilon\varepsilon_o^2\ \zeta\Delta p\ r^2 / \mu L. \quad (8)$$

The flow rate of the uncompensated charge Q = Q (t) through the "real" flow section is dQ/dt = I – i, where $i = Q/\varepsilon\varepsilon_0^2\lambda$ is the conduction current determined by the specific electric resistance of the fluid λ (for mineral oil $\lambda = 1\times10^7$ kOhm× m). Thus, the flow rate of the uncompensated charge will be determined by the equality:

$$dQ / dt = \pi\varepsilon\varepsilon_o^2\zeta\Delta p\ r^2 / \mu L - Q / \varepsilon\varepsilon_o^2\lambda. \quad (9)$$

Temporal integration of charge consumption (9) determines its accumulated value:

$$Q(t) = \pi\varepsilon^2\varepsilon_o^4\zeta\lambda\Delta\ p\frac{r^2}{\mu L}\left[1 - \exp\left(-t / \varepsilon\varepsilon_o^2\lambda\right)\right]. \quad (10)$$

For $t \to \infty$ and $dQ/dt \to 0$ the accumulated charge Q becomes equal

$$Q_\infty = \pi\varepsilon^2\varepsilon_o^4\ \zeta\lambda p\ r^2 / \mu L. \quad (11)$$

This charge determines the electric field near the solid wall $E = Q/4\pi\varepsilon\varepsilon_0^2 r\ L$ and the stationary charge density:

$$\sigma = 2E\varepsilon\varepsilon_o^2 = Q_\infty / 2\pi r\ L\ . \quad (12)$$

Will give a theoretical estimate of the values of the accumulated uncompensated charge Q_∞(11) and the stationary charge density (12) for the investigated transparent throttle modules.

Diaphragm throttle

Source data:

$r = 0{,}5\times 10^{-3}$ m; $L = 0{,}5 \times 10^{-3}$ m; $\varepsilon = 2{,}2$; $\varepsilon_0 = 8{,}85 \times 10^{-12}$ F·m^{-1}(Farads per meter); ζ= 1V;

$\lambda = 1\times 10^7$kOhm×m; μ= 170 kg/ms; Δp = 3 MPa.

Calculation results: $Q_\infty = 1{,}4\times 10^{-10}$ C(Coulomb); $\sigma = 0{,}9 \times 10^{-4}$C/m^2.

Capillary throttle

Source data:

$r = 1\times 10^{-3}$ m; $L = 25\times 10^{-3}$ m; $\varepsilon = 2{,}2$; $\varepsilon_0 = 8{,}85 \times 10^{-12}$ F·m^{-1}(Farads per meter); ζ= 1V;

$\lambda = 1\times 10^7$kOhm×m; μ= 170 kg/ms; Δp = 3 MPa.

Calculation results: $Q_\infty = 0{,}11\times 10^{-10}$ C (Coulomb); $\sigma = 0{,}9 \times 10^{-6}$C/m^2.

As it follows from the calculation results, the accumulated uncompensated charge in the diaphragm control throttle is 12,5 times higher and the stationary density is in 100 times higher than in the capillary one.

The expression in square brackets of equality (10) determines the attenuation decrement of the process of increasing the flow rate of an uncompensated charge and is 0,37 s^{-1}. For a time $t \approx 2, 7$ s, due to the draining of the resulting charge and in accordance with equality (10), the damping ratio decreases 2,7 times. During this time, in the cavitation flow of mineral oil an explosion of a cavitation bubble filled with a vapor-air mixture can occur. The explosion voltage of the bubble is much less than the critical tension of mineral oil which can cause light emission at the input edge of the diaphragm throttle.

The stationary charge density in the capillary throttle is 100 times less than in the diaphragm throttle, therefore, light emission is not observed. The composition of the vapor bubble is closely related to the base of mineral oil and a set of corrective additives. Due to this, with identical parameters of the cavitation flow light emission at the inlet edge of the diaphragm throttle may not be observed [25 - 27].

A comparative analysis of the flow parameter graphs (Fig. 2a and 2b) and the range of electrical signals (Fig. 5 ... 9) shows that the electrical signals in the module leads become observable at numbers $Re > 0.25 \times 10^4$.

List of reference

[1] Wave Processes Regulators Optimisation in Hydraulic Systems D N Popov, N G Sosnovsky and M V, Siukhin 2018 *IOPConf. Ser.: Mater. Sci. Eng.* **468** 012014.htpps://iopscience.iop.org/issue/1757-899X/468/012014.

[2] Margulis M.A. Sonochemistry and cavitation. Gordon & Breach, London, 1995. — 543 p.

[3] Bagrov V.V., Desiatov A.V. and others. Water: effects and technologies. Publishing House ONIC "Engineer", LLC "Oniko-M", M. — 2010, 488 p.

[4] Gertsenshtein S. IA.Monakhov A. A. Electrification and fluorescence of a fluid in a coaxial channel with dielectric walls. Fluid Dynamics A Journal of Russian Academy of Sciences, No. 3, M. — 2009, p. 114–119.

[5] Margulis M.A., Pilgunov V.N. About the mechanism of occurrence of luminescence and electrification during the flow of liquids in a narrow channel. Journal of Physical Chemistry, Volume 83, No. 10, M. — 2009, p. 1975–1979.

[6] Koldomasov A.I. Plasma formation in cavitating dielectric fluid. Journal of Theoretical Physics. Volume 61, M. — 1991, p. 256–263.

[7] Vysotskii V. I. and others. The generation of intense directional emission during the rapid movement of a jet of liquid through dielectric channels. Fluid Dynamics A Journal of Russian Academy of Sciences. Surface. X-ray, synchrotron and neutron studies. No. 3, — 2007, p. 55–60.

[8] IA. I.Frenkel. About electrical phenomena associated with cavitation due to ultrasonic vibrations in a liquid. Journal of Physical Chemistry, Volume 14, M. — 1940 p. 305.

[9] M.A. Margulis. The study of electrical phenomena associated with cavitation. Journal of Physical Chemistry, Volume 55, M. — 1981, p. 154–158.
[10] Ring-shaped fluorescence of mineral oil on the front edge of the choke coil V Pilgunov and K Efremova 2019 *IOPConf. Ser.: Mater. Sci. Eng.* **492** 012028. htpps://doi.org/10.1088/1757-899X/492/1/012028.
[11] Measurements of acoustic flow parameters in the orifice on non — linear regimes. A Bykov, A Komkin and V Moscalenko 2019 *IOPConf. Ser.: Mater. Sci. Eng.* **589** 012015. htpps:// iopscience.iop.org/issue/1757-899X/589/1/012015.
[12] M.A. Margulis. Electrical phenomena during the explosion of cavitation bubbles. Journal of Physical Chemistry, Volume 71, M. — 1997, p. 1885–1889.
[13] Independent component analysis of hydrodynamic bubbles propertiesSGavrilov, O Ivanova and T Decaen 2019 *IOPConf. Ser.: Mater. Sci. Eng.* **492** 012014. htpps://doi.org/10.1088/1757-899X/492/1/012014.
[14] Regulation of bubbles descending speed in water. B Ksenofontov, M Ivanov, S Shauhan and I Schaikhiev 2019 *IOPConf. Ser.: Mater. Sci. Eng.* **492** 012023. htpps://doi.org/10.1088/1757-899X/492/1/012023.
[15] Analysis of hydrodynamic properties of a gas phase in water by hydroacoustic method. S Gavrilov and M Ivanov 2019 *IOPConf. Ser.: Mater. Sci. Eng.* **492**012030. htpps://doi.org/10.1088/1757-899X/49 2/1/012030.
[16] M.A. Margulis, I.M. Margulis. Electrical phenomena on the surface of pulsating cavitation bubbles. Journal of Physical Chemistry, Volume 71, M. — 1997, p. 1890–1895.
[17] C.V. Seghal, R.E. Verral. A review of the Electrical Hypothesis of Sonoluminescens, Ultrasonics,V.20, 1982, p. 37–39.
[18] T. Lepoint, D. De Pauv, F. Lepoint-Mullie, M. Goldman. Sonoluminescens: an Alternative Electrodynamic Hypothesis, *J. Acoust. Soc. Amer.*, V. 101, 1997, p. 2012–2030.
[19] Sonoluminescence. Milia A Margulis 2000 *Phys.-Usp.* **43** 259. https://doi.org/10.1070/PU2000v043n03ABEH000455
[20] Sonoluminescence and acoustic cavitation Pak-Kon Choi 2017 *Jpn. J. Appl. Phys*.**56** 07JA01. https://doi.org/10.7567/JJAP.56.07JA01.
[21] M.A. Margulis, I.M. Margulis. Theory of Local Electrification of Cavitation Bubbles: New Approaches. Sonochemistry, V. 6, 1999, p. 15–20.
[22] Research of centrifugal gas-liquid separator G Budaev, D Danilov, A Kuznechov, V Lomakin and V Cheremushkin 2019 *IOPConf. Ser.: Mater. Sci. Eng.***589** 012035. htpps: // iopscience.iop.org/issue/1757-899X/589/1/012035.
[23] Electric Characteristic and cavitation bubble dynamics using under water pulsed discharge. Minglei SHAN. Bingyan CHEN. Cheng YAO. Qingbang HAN. Changping ZHU and Yu YA/ 2019 *Plasma Sci.Technol.* **21** 074002. https://doi.org/10.1088/2058-6272/abOb62.
[24] Electrical pulses produced by cavitation bubbles G.Gimenez 1979 *J.Phys.D: Appl. Phys.* **12** L25. https://doi.org/10.1088/0022-3727/12/4/001.
[25] E. Kh. Isakaev, A. S. Tyuftyaev, M. Kh. Gadzhiev, N. A.Demirov and P. L. Akimov. Influence of ultrasound on the electrical breakdown of transformer oil. 2018 *J. Phys.: Conf. Ser*.**946**012175. https://doi.org/10.1088/1742-6596/946/1/012175.
[26] Measurement of near-wall stratified bubbly flows using electrical impedance. J Cho. M Perllin and S I Ceccio 2005 *Meas. Sci. Technol* **16** 1021. https://doi.org/10.1088/0957-0233/16/4/015.
[27] A liquid dielectric in an electric field. Mikhail N Shneider and Mikhail Pekker. Pages 4-1 to 4-30. Chapter 4 from Liquid Dielectrics in an Inhomogeneous Pulsed Electric Field (Second Edition).